ORIGINAL PAPER

Influence of Base oil Polarity on the Tribological Performance of Surface-Active Engine Oil Additives

Febin Cyriac[1] · Tee Xin Yi[1] · Sendhil Kumar Poornachary[1] · Pui Shan Chow[1]

Abstract

Friction, wear and tribofilm growth of organic friction modifiers (glycerol monooleate and oleamide), anti-wear additive (ZDDP) and binary additive system comprising the organic friction modifiers and ZDDP were studied in polyalphaolefin (PAO) and ester oil. The mechanisms underlying base oil polarity-dependent frictional performance of the OFM and AW additives at high temperature (140 ℃), either singly or in combination, were investigated in the light of chemical composition analysis of the tribofilms post friction measurements using energy dispersive X-ray spectroscopy (EDX), static and dynamic time-of-flight secondary ion mass spectrometry (ToF–SIMS). Depending on the rubbing conditions, the boundary friction coefficient of the binary additive systems was found to be either lower than that of individual additives or to lay between the values for the individual additives. Chemical composition analysis of the tribofilms indicated that the nature of base oil controlled interactions between ZDDP and OFM and consequently adsorption and reactive tribofilm formation in the boundary lubrication layer. Surface roughness and wear scar width measured post tribological tests using 3D surface profiler showed improved wear performance in both PAO and ester-based additive formulations.

Keywords Friction · Organic friction modifier · ZDDP · ToF-SIMS

1 Introduction

The use of lubricants dates back to thousands of years and has played a pivotal role in enhancing the durability and efficiency of mechanical components. Lubricants used today have complex chemical makeup where a variety of bulk and surface-active additives are added to the base oil. Lubricant additives enhance the inherent properties of the base oil and also impart new characteristics to improve the performance [1]. A significant amount of energy is lost to parasitic frictional losses in internal combustion engines where a piston-cylinder system accounts for 40–55% of total energy losses [2]. Therefore, one of the main objectives of using lubricants in automotive environment is to improve the fuel efficiency by keeping a check on frictional losses at tribological contacts. The need for improved energy efficiency has led to the shift toward low viscosity lubricants [3]. Even though low

viscosity lubricants contribute to improved energy efficiency by reducing fluid friction, they are likely to cause a break in oil film. The decrease in base oil viscosity will lead to a decrease in film thickness eventually reaching that of composite surface roughness resulting in high friction and wear in boundary/ mixed lubrication regimes. Therefore, friction modifiers and anti-wear additives are used in commercial systems to enhance engine oil performance and to meet ever-rising automotive industry demands.

The state-of-the-art boundary lubricant additives include organic friction modifiers (OFMs) and zinc dialkyldithiophosphate (ZDDP), an anti-wear additive. Considerable research has been carried out to understand the mechanism of action of organic friction modifiers. Friction reduction by OFMs is related to formation of either a monolayer film [4–6] or a thick viscous film [7–10] that prevents metal-to-metal contact. The amphiphilic molecules, either physisorb or chemisorb on to the metal surface, are difficult to compress but can easily be sheared off at the hydrocarbon tail interface leading to reduced friction and adhesion [11]. Most commonly used OFMs include oleamide (a reaction product of olein and ammonia) and glycerol monooleate (GMO, a reaction product of glycerin and olein) [11, 12].

✉ Febin Cyriac
febin_cyriac@ices.a-star.edu.sg

1 Institute of Chemical and Engineering Sciences, Agency for Science, Technology and Research (A*STAR), 1 Pesek Rd, Singapore 627833, Singapore

Early studies have shown that GMO and oleamide exhibit high friction reducing properties over a wide range of temperature where optimum performance was observed at 70 ℃ [13]. In general, oleamide was found to be more effective in reducing friction than GMO [14, 15]. These unsaturated acids were found to exhibit enhanced friction reducing properties despite their inability to form close-packed monolayer structures [16]. Molecular dynamics simulation suggests that they allow less lubricant interdigitation than acid OFMs and therefore lower friction coefficients [3].

A substantial amount of studies has been devoted to understand the multifunctional mechanism of ZDDP as an anti-oxidant and anti-wear agent [15, 17–19]. ZDDP reduces wear by decomposing at the contact interface to form reactive films with hardness characteristic of soft polymeric materials [20]. The sacrificial boundary films thus formed on the surface suppress surface wear by preventing asperity interactions. A number of factors, such as base oil characteristics (polarity), competing additives, contaminants, metallurgy and temperature, can influence the effectiveness of the surface-active additives [11, 21]. A number of studies have focused on the tribological performance competing additives. From the overview of data available in the literature, it is evident that when two different additives are combined in a solution they may behave synergistically, antagonistically or in some cases one additive may predominate over the other, while in some cases friction may lie between the values shown by either additives [14, 22–31].

Severely hydro-treated base oils, polyalphaolefin (PAO) and ester oil are gaining market attention due to their advantages over Group I and Group II oils in terms of viscosity index, volatility, pour point, etc. [32]. As the effectiveness of OFMs on a given surface can be highly variable depending on the nature of base oil, their mechanism of action in different oils needs investigation. However, the influence of base oil on the tribological performance of surface-active additives has hardly been addressed. Some studies have shown that base oil polarity influences the transport of additives from bulk medium to the metal surface [33, 34]. The diffusivity of additives can in turn influence their adsorption kinetics and thereby tribological performance. The aim of the present study is to elucidate the influence of base oil polarity on the tribological performance of industry relevant OFMs and ZDDP. Currently, we do not have a systematic understanding of how friction modifiers interact with other surface-active additives in base oil of different polarity.
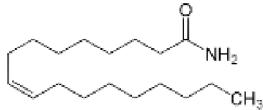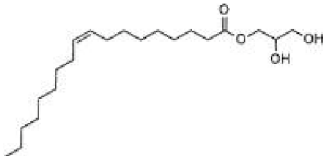
A ball-on-disc tribometer was used to measure the frictional performance of these additives formulated in PAO (Group IV) and ester (Group V) oil. The effectiveness of the additives to form a tribofilm was studied using a 3D Spacer Layer Imaging Method (SLIM). Scanning electron microscope (SEM) coupled with energy dispersive X-ray spectroscopy (EDX) was used to investigate the morphology and elemental composition of additive films adsorbed on the metal surface post tribological tests. As information concerning the nature and structure of the film are important for understanding the lubrication mechanism, chemical composition of thin film formed on the friction surface was investigated using ToF–SIMS. The wear track width on the disc specimens was analysed ex situ using a 3D surface profiler. Tribological mechanism of the above additives in base oils of different polarities is discussed based on the experimental results.

2 Experimental Details

2.1 Materials

Oleamide and glycerol monooleate were used as model friction modifiers due to their practical relevance as engine oil additives (Table 1). A mixed primary and secondary alkyl ZDDP was used as anti-wear additive. Metallocene PAO 6 (with viscosity 24.8 mPa s at 40 ℃ and 4.35 mPa s at 100 ℃)

Table 1 Tested lubricants

1. PAO	2. Ester oil	
3. PAO + 0.5 % GMO	4. Ester oil + 0.5 % GMO	
5. PAO + 0.5 % Oleamide	6. Ester oil + 0.5 % Oleamide	Oleamide
7. PAO + 0.2 % ZDDP	8. Ester oil + 0.2 % ZDDP	
9. PAO + 0.5 % GMO + 0.2 % ZDDP	10. Ester oil + 0.5 % GMO + 0.2 % ZDDP	
11. PAO + 0.5 % Oleamide + 0.2 % ZDDP	12. Ester oil + 0.5 % Oleamide + 0.2 % ZDDP	GMO

and monoester oil (Non Polarity Index—214) with viscosity of 21.6 mPa s at 40 ℃ and 4.29 mPa s at 100 ℃ were used as the base oil. It is known that the use of low NPI ester oil can promote seal swell and therefore is only used at low dose rate (5–15%) to enhance additive solubility and to improve viscosity index in commercial engine oils. We employed ester oil of high NPI as they are recommended for practical application due to the above-mentioned limitation associated with low NPI ester oils. Viscosity of ester oil and PAO measured with a double gap geometry using an Anton Paar 702 rheometer at the test temperature (140 ℃) was found to be 2.44 ± 0.1 mPa s and 2.38 ± 0.2 mPa s respectively. As the viscosities of PAO and ester oil are similar, the observed frictional response can be attributed to the structural aspects of the additives and/or difference in base oil polarity.

Lubricant oil formulations were prepared by dissolving 0.5 wt% of OFM at 60 ℃ under stirred conditions, while the concentration of ZDDP was kept at 0.2 wt% in all the formulations. Table 1 shows the additive/base oil combinations used for tribological performance evaluation. Since oleamide solutions in PAO showed visible precipitates at room temperature (23 ℃), the tribology tests were performed immediately after sample preparation. As no precipitates were observed during sample preparation at 60 ℃, by monitoring the turbidity of the solution for a certain period of time, it can be reasoned that the additives remain dissolved in the base oil during the tribological measurements at 140 ℃.

2.2 Determination of Particle Size

The particle size of single and binary additive systems in both PAO and ester oil was determined from dynamic light scattering (DLS) data using Malvern Panalytical Zetasizer nano equipment. Measurements were carried out in a quartz glass cuvette using 1.5 ml sample. The Z-Average particle size was determined at 90 ℃, the limiting operating temperature of the equipment.

2.3 Tribological Characterization

Tribological measurements were carried out using the MTM ball-on-disc tribometer (PCS Instruments, UK) equipped with a 3D surface mapper (SLIM). AISI 52100 steel ball

(radius 9.525 mm) on disc with surface roughness 20 and 10 nm, respectively, was used as the tribo-pair. The measurements were carried out at 140 ℃. It should be noted that most of the earlier studies on ZDDP and OFMs were performed at temperatures 100 ℃ and below [14, 16–18, 22, 35]. A higher temperature was chosen to accelerate the generation of chemically reacted film which is known to depend on the severity of tribological contact [36]. As temperature plays an important role with regard to adsorption/desorption phenomena, measurement at higher temperature can be used for identifying product groups that are most effective under more severe requirements with regard to friction retention.

Tribological measurements are repeated twice and were carried out in three distinct phases (Table 2). First, the ball and disc were rubbed at an entrainment speed of 100 mm/s at 100% slide roll ratio (SRR) to generate the tribofilm. Under these conditions, from the lambda ratio, it was found that the contact operated under the boundary lubrication regime. Rubbing was followed by optical film thickness measurement using SLIM (spacer layer interferometry) where a high-resolution, RGB CCD colour camera was used to grab images of the contact. Here, film thickness was calculated by matching the colours in the image to a previously determined colour space calibration. One limitation of SLIM technique is accurate value of refractive index is needed for converting measured optical film thickness to true film thickness. Due to the practical difficulty in obtaining refractive index of tribofilm formed by different additives and its combination, true film thickness was estimated by using a single value of 1.47 as the refractive index for all samples. Lastly, Stribeck curves were measured in the speed range between 2000 and 1 mm/s. During Stribeck curve measurements, the frictional force is measured in both directions. This is achieved by maintaining the same mean speed, but reversing the sign of the SRR. For the first measurement, the disc speed is three times greater than the ball speed, whereas for the second measurement the disc speed is one-third of the ball speed. The rolling speed is calculated from the average of the first and second measurements.

2.3.1 Surface Characterization

ToF–SIMS analysis of tribofilms formed on the MTM disc surface after 120 min of rubbing was performed with ToF.

Table 2 Test protocol used for tribological characterization

Phase	Load (N)	Pmax (GPa)	Speed range (mm/s)	SRR (%)	Temperature (℃)
Preconditioning	36	1.0	100	100	140
Tribofilm measurement	36	0.57	–	–	140
Stribeck curve measurement	36	1.0	2000–1	100	140

SIMS 5 (ION-TOF, Münster, Germany) instrument and the spectra obtained were processed using IonSpec software. Prior to surface characterization, ToF- SIMS spectra of the base oil, GMO, oleamide and ZDDP samples were also collected for reference. The instrumental parameters and measurement protocol used for the static and dynamic analysis of the disc specimens are discussed elsewhere [36]. Further, elemental composition of tribofilm formed on the wear surface was carried out using JEOL JSM-7900F field emission scanning electron microscope (FESEM) equipped with Oxford INCA energy dispersive X-ray (EDX) spectrometer. The measurements were carried out at a beam voltage of 10 keV and the spectral images were acquired at ×160 magnification. Wear analysis was carried out using Infinite Focus Alicona benchtop optical 3D surface profiler. Surface analysis was preceded by rinsing the metal disc in *n-hexane* to remove the residual oil and contaminants sticking to the surface.

3 Results and Discussion

The DLS data for single and binary additive systems are discussed first. This is followed by Stribeck curve measurements and SLIM results for neat ester and PAO base oils. Next, friction measurements of the base oils formulated with friction modifiers (GMO and Oleamide) and anti-wear additive (ZDDP) are discussed. Finally, the influence of base oil polarity on the binary additive system comprising both OFM and AW additives is studied. The tribological mechanism is discussed under relevant sections by correlating insights obtained from surface analysis (SEM–EDX and ToF–SIMS) and friction measurements. Finally, the impact of base oil polarity on the wear performance of the above additives is summarized.

3.1 Size of Dispersed Particles

The Z-average particle size obtained for the single and binary additive systems in PAO and ester oil are shown in Table 3. Among different additives, ZDDP resulted in smaller particles in both PAO and ester oil. This may be due to lower concentration of ZDDP used in the formulations. A distinct influence of base oil polarity on the particle size of dispersed phase is evident from DLS data. Here, irrespective of the type of additives or their combinations, a higher particle size was observed in non-polar PAO. The result suggests that polar additive molecules can readily disperse in polar oil creating smaller size particles than in non-polar oils. Further, an increase in Z-average particle size was observed for the binary additive systems in both polar and non-polar oil. This may be an indication that OFMs and ZDDP self-assembled to form nano- to micro-scale structures of varying sizes or

Table 3 Z-Average size and standard deviation obtained from five measurements for different additives in PAO and ester oil

Additives	Z-Average size (nm)	
	PAO	Ester oil
0.5% GMO	1388 ± 219	318 ± 85
0.5% Oleamide	915 ± 141	374 ± 24
0.2% ZDDP	163 ± 11	157 ± 36
0.5% GMO + 0.2% ZDDP	1597 ± 265	908 ± 196
0.5% Oleamide + 02% ZDDP	1033 ± 249	488 ± 34

some particles might have moved closer to each other in the binary system leading to an increase in particle size. However, we did not investigate this aspect in detail. In order to discern the influence of particle size on the tribological performance, the Z-average size from DLS was compared with the boundary friction coefficient (BFC) from Fig. 4. However, the result suggest that these two parameters are poorly correlated ($R^2 = 0.63$ for 5 min rubbing and $R^2 = 0.69$ for 120 min rubbing).

3.2 Friction Measurements in Neat PAO and Ester Oil

Figure 1i and ii shows the optical interference images obtained after rubbing the ball–disc contact for predefined period of time in PAO and ester oil. The light blue images obtained at 0 min is due to the space layer alone, while it changed to dark blue as the film developed during rubbing. However, the interference fringes indicate the presence of viscous liquid film for both PAO and ester oil. The viscous film is due to local entrapment of oil where the exponential increase in viscosity with pressure could have prevented the oil from flowing out of the contact [37, 38]. Some film deposition is observed after prolonged rubbing for the neat base oils. For ester oil the film was found to grow continuously close to the upper side of SLIM image than the central region. As precipitates from thermal degradation can lead to such deposition, absorption mode Fourier Transform Infrared Spectroscopy (FT-IR) (using a PerkinElmer Frontier FT-IR/NIR spectrometer) and viscosity measurements of tribo-tested oils were carried out to study the likelihood of oxidative degradation. Oxidation peak suggesting oil degradation was not observed under FT-IR for the tribo-tested oils Fig. 2. An earlier study found that PAO and di-ester oil are thermally stable up to 200 and 300 ℃, respectively [39]. But, an increase in viscosity of 1.35% for PAO and 2.1% for ester oil was observed, suggesting oil degradation of some sort. By reverse loading the ball against the mapper disc, horizontal scratches suggesting wear could be observed from the optical interferograms with the signs of wear more apparent in ester oil. The latter phenomenon was also evidenced from
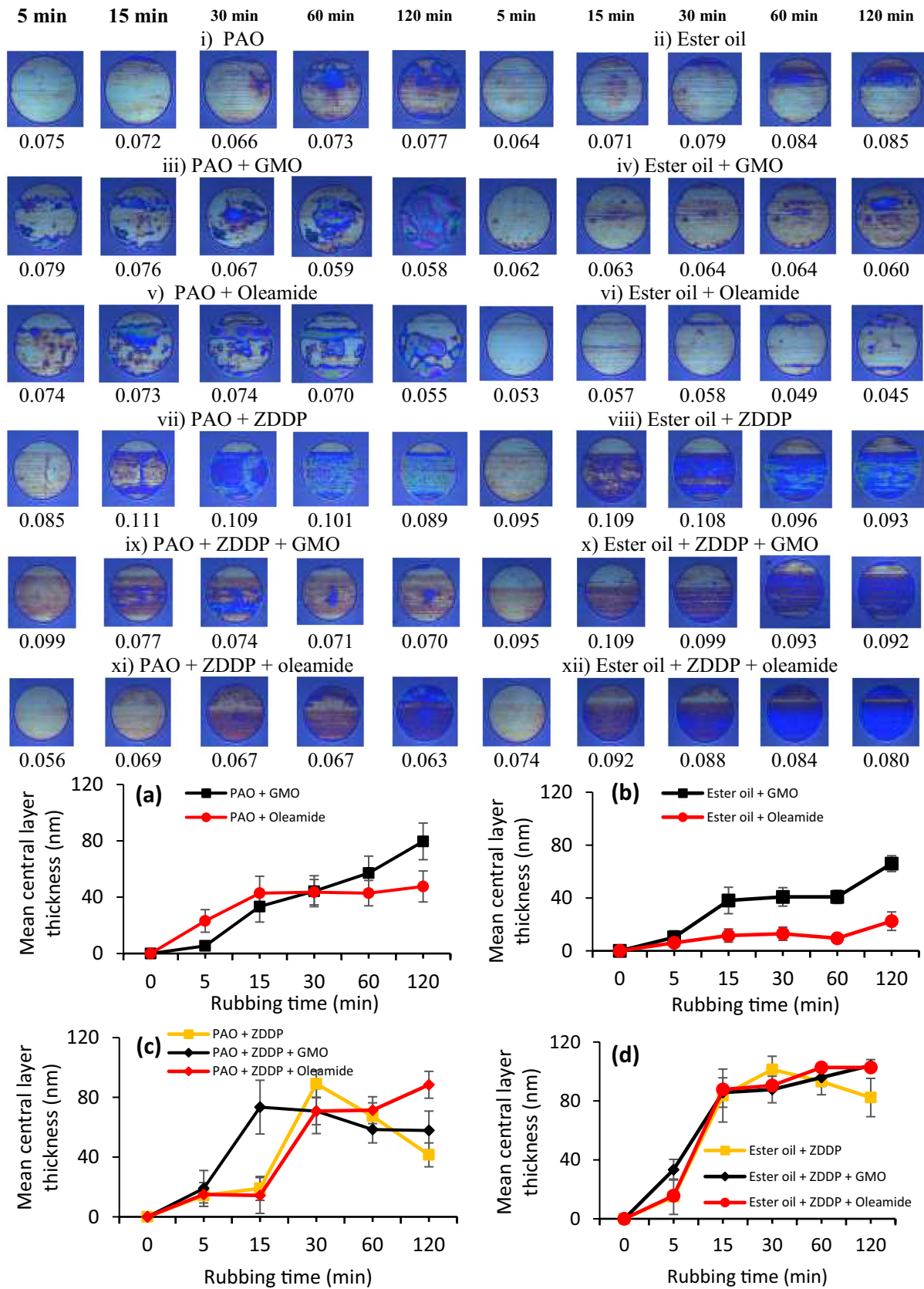
Fig. 1 Optical interferograms and mean film thickness along the axis of the contact for different additives after different rubbing durations. Average friction values measured for different rubbing durations during the preconditioning phase are also shown under each optical interferograms
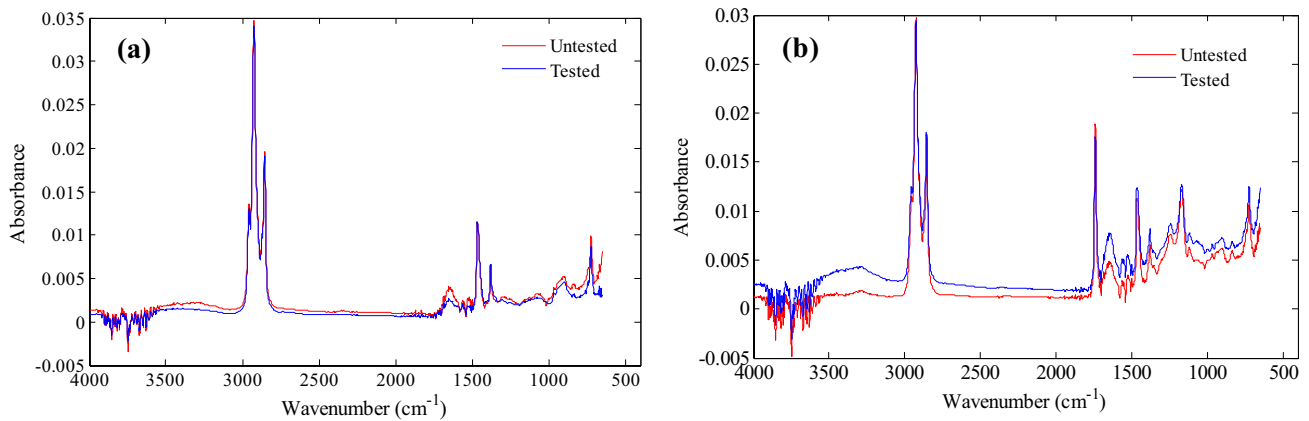
Fig. 2 FT-IR data for tested and untested samples, **a** PAO and **b** ester oil

disruption of the Hertzian contact from perfect circle after 60 min of rubbing.

The Stribeck curves obtained in PAO and ester oil are shown in Fig. 3a and b. An increased rubbing time constituted to an increase in friction in both the base oils, which can be attributed to topographical changes due to wear at the contact interface. This is also evident from friction coefficient measured during the preconditioning phase, where prolonged rubbing was found to increase the friction (Fig. 1i and ii). Boundary friction coefficients obtained at the same rubbing duration are compared in Fig. 4. Irrespective of the rubbing duration, PAO exhibited a higher boundary friction coefficient than ester oil. The higher lubricity observed for ester oil can be due to its ability to adsorb more favourably on to the metal surface than PAO.

Figure 5a and b shows high-resolution SEM images of the wear surfaces and the corresponding elemental analysis at three different locations for PAO and ester oil. A uniform surface smearing with abrasion grooves and traces of adhesive wear along the rolling direction are apparent for both the oils. Nevertheless, ester oil-based disc surface shows sign of higher abrasive wear which agrees with the observation by optical interferometry. SEM images also show darker regions near the edge of the wear scar characterized by higher concentration of oxygen and carbon. This was found to be more distinct for ester oil than PAO. It is known that frictional heating and the resulting contact temperature can lead to oxidation of surface and often influence the behaviour of lubricant present in the contact [40, 41]. Therefore, it is hypothesized that transient flash temperature rise due to contact spots between surface roughness peaks resulted in the formation and deposition of precipitates from the base oil that are below the detectable limit of FT-IR. Other than the darker patches, the frictional surface showed no notable difference in concentration of carbon and oxygen within and outside the wear surface.

For the ToF–SIMS spectra obtained in the positive and negative ion modes of the worn surfaces, mass fragments attributed to PAO (C_nH_{2n-3} to C_nH_{2n+1}) and ester oil ($[C_7H_{13}O_2]^-$, $[C_{18}H_{35}O_2]^-$ etc.) [42] were evident (results not shown). In general, the peaks corresponding to ester oil were found to be of higher intensity compared to PAO, indicating higher affinity of ester molecules on steel surface. However, it is possible that hexane (non-polar solvent) removed more PAO from the surface when the metal disc was washed prior to surface analysis. This could also be a reason for observing lower intensity peaks in the case of PAO.

3.3 Influence of Base Oil Polarity on the Tribological Performance of GMO

As shown in Fig. 1a and b, the tribofilm thickness increased in a continual and gradual manner reaching a film thickness of 80 and 66 nm, respectively, in PAO and ester oil after 120 min rubbing. However, in PAO, the morphology of tribofilm did not appear to be typical of other surface-active additive films. Here interference fringes that are characteristic of viscous liquid film was observed (Fig. 1iii). The viscous film could have been transferred to the SLIM glass disc by the ball, augmented during the subsequent measurements as evidenced from the optical images. Thicker films observed for GMO in PAO could be a manifestation of this effect. Unfortunately, it was not possible to decouple the contribution of viscous film from the total film thickness. Notwithstanding this observation, the decrease in friction during the preconditioning phase (Fig. 1) and a decrease in boundary friction coefficient (BFC) with rubbing time for GMO-containing oils (Fig. 4) could indirectly imply the presence of an additive film beneath the viscous oil film. The large error bars associated with the mean layer thickness for GMO may create an impression of large variations in film thickness across the rubbed track. But this was found to be
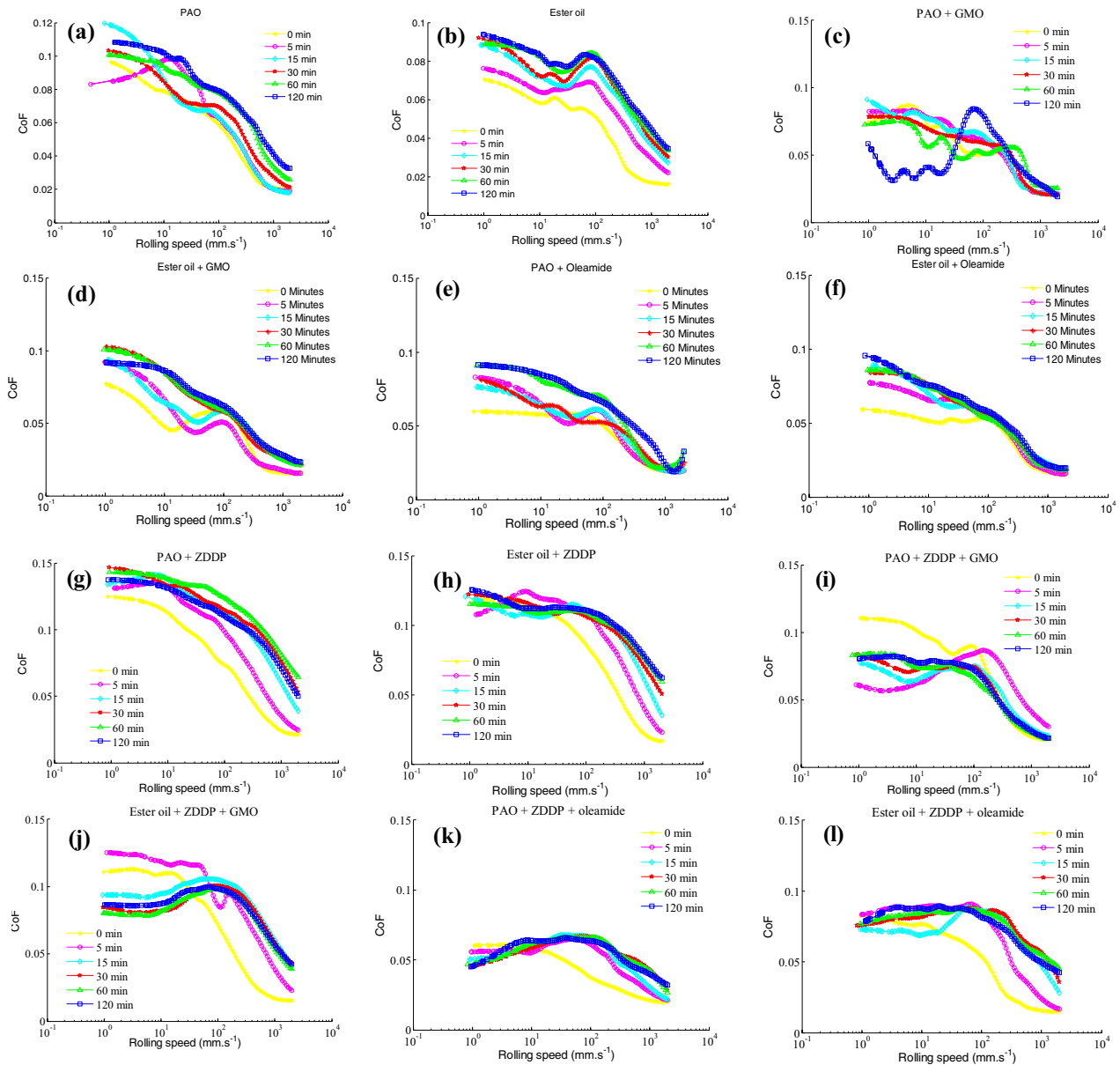
Fig. 3 Influence of rubbing time on Stribeck curves for different additives in PAO and ester oil

mainly contributed by the variation in viscous film that was transferred to the coated glass disc by the steel ball.

The Stribeck curve for GMO-based oils are shown in Fig. 3c and d. Addition of GMO to PAO contributed to a decrease in friction with rubbing time. In contrast, extended rubbing resulted in an increase of friction in ester oil. A decrease in CoF for PAO + GMO formulation underlines GMO to be an effective friction reducing agent in non-polar oil. This is also reflected in Fig. 4 where a significantly lower BFC is observed for GMO-containing oil compared to neat PAO. At rolling speed below 10^2 mms^{-1}, the Stribeck curve for PAO + GMO shifts to a significantly lower value of boundary friction after 120 min

of rubbing. This observation suggests the formation of a thick GMO tribofilm. A similar phenomenon was observed earlier for GMO in GIII base oil under similar rubbing conditions [36]. In the boundary lubrication regime, GMO exhibited a marginal improvement in friction in ester oil compared to base stock (Fig. 4). It is hypothesized that, in ester oil, GMO molecules have to compete heavily with ester molecules to be adsorbed on the metal surface. It is likely that the competition between ester molecules and GMO could have resulted in higher asperity contact spots within a nominal contact patch than in PAO. Much thinner tribofilms and correspondingly higher BFC observed for GMO + ester oil supports this notion. This corroborates
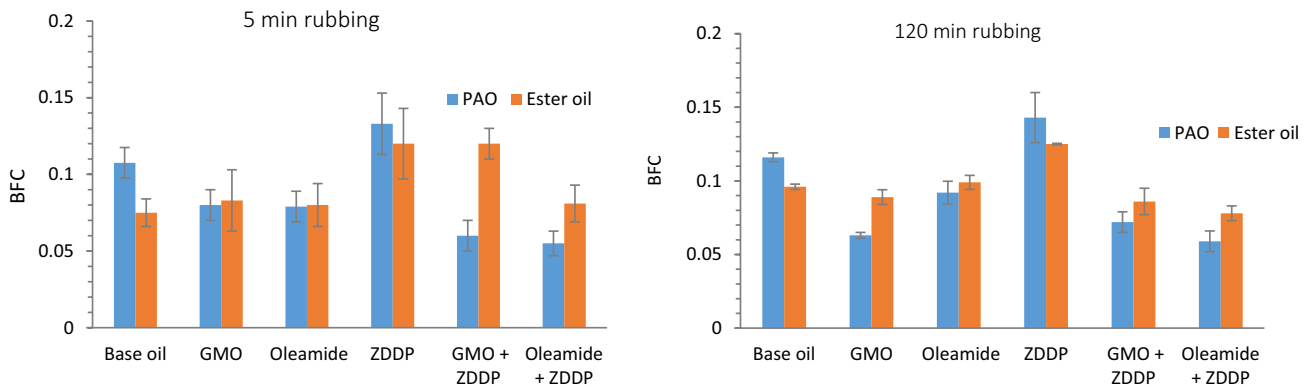
Fig. 4 Average boundary friction coefficient of different additives in PAO and ester oil after 5 and 120 min rubbing. The average friction values in the speed range of 1 to 10 mm/s from two different measurements were taken as the BFC

with the SEM–EDX data shown in Fig. 5c and d. Thin abrasion grooves along the rolling direction are apparent in the case of ester oil + GMO, whereas wear scratches are not apparent for GMO in PAO. EDX data showed higher concentration of carbon and oxygen within the wear track lubricated with PAO + GMO, which can be attributed to the adsorption of GMO on the surface, as observed from visible deposits of GMO. This suggests the presence of a 'solid-like' film beneath the viscous film shown in the optical interferograms (Fig. 1). In the case of ester oil + GMO, no notable difference in carbon/oxygen composition is observed within and outside the wear track. A lower concentration of carbon and oxygen on the frictional surface (EDX data) and a much thinner tribofilm (optical interferometry) suggest that GMO has to compete with the polar base oil to get adsorbed on the steel surface.

To ascertain the tribological mechanism is in action, the chemical nature of tribofilm was analysed using static ToF–SIMS. Hydrocarbon species with a general formula $[C_nH_m]^+$ were observed in the positive ion spectra (results not shown). Ions corresponding to $[C_{17}H_{33}COO]^-$, which indicates chemisorption of GMO molecule [43, 44], and ionic species, such as $[C_{17}H_{33}O_3]^-$, $[C_{18}H_{33}O]^-$, $[C_{16}H_{31}O]^-$ and $[C_{16}H_{29}O]^-$ [45], formed by interaction of cleaved alkyl tails of GMO with oxygen at the iron oxide surface, suggesting decomposition of GMO, were observed on the surface (Fig. 6a). However, quasi-molecular ions corresponding to iron alkoxalate $[CH_3OFe]^+$, suggesting reaction of GMO decomposition products on the friction surface, was not observed in both the oils. It is noted that both the additive and base oil are composed of hydrogen, carbon and oxygen, and hence, the ToF–SIMS peaks can be attributed to adsorption of GMO and/or the hydrocarbon molecules in base oil (Fig. 6). In view of this ambiguity, it is difficult to ascertain the contribution of GMO alone to the total peak intensity.

3.4 Influence of Base Oil Polarity on Tribological Performance of Oleamide

Optical interference images and the corresponding film thickness maps acquired at different rubbing durations for oleamide solutions in PAO and ester oil are shown in Fig. 1 (see v, vi, a and b). In general, oleamide formed a thinner film than GMO in both the oils. This suggests that GMO is a more effective surface film-forming additive than oleamide. Irrespective of the thinner film being formed, oleamide-based samples offered better friction reduction than GMO-based samples during the preconditioning phase (Fig. 1). Optical interferograms show much thicker films for oleamide in PAO, but interference fringes typical of viscous films are apparent which can contribute to total film thickness. Horizontal scratches indicative of wear can be observed for oleamide in ester oil. However, the scratches formed are found to be less severe compared to that observed for ester oil alone.

Figure 3e and f shows the Stribeck curves for oleamide in PAO and ester oil, respectively, acquired after different rubbing durations. Prolonged rubbing constituted to an increase in boundary friction for both the oils, which can be attributed to topographical changes at the contact interface due to wear. But it should be noted that any adsorbed species or precipitates in the contact zone can also contribute to the observed increase in the friction coefficient, as they can hinder the entrainment of the lubricating oil into the contact [46]. Comparing PAO and ester oil, for the latter rubbing had little effect on the friction at intermediate and high speed. Therefore, it is believed that any adsorbed species within or at the vicinity of contact zone did not deter lubricant entrainment in the mixed lubrication regime. At a given rubbing time, addition of oleamide to PAO had a positive effect on the frictional performance (Fig. 4). Oleamide in ester oil also had a positive effect, but the influence was
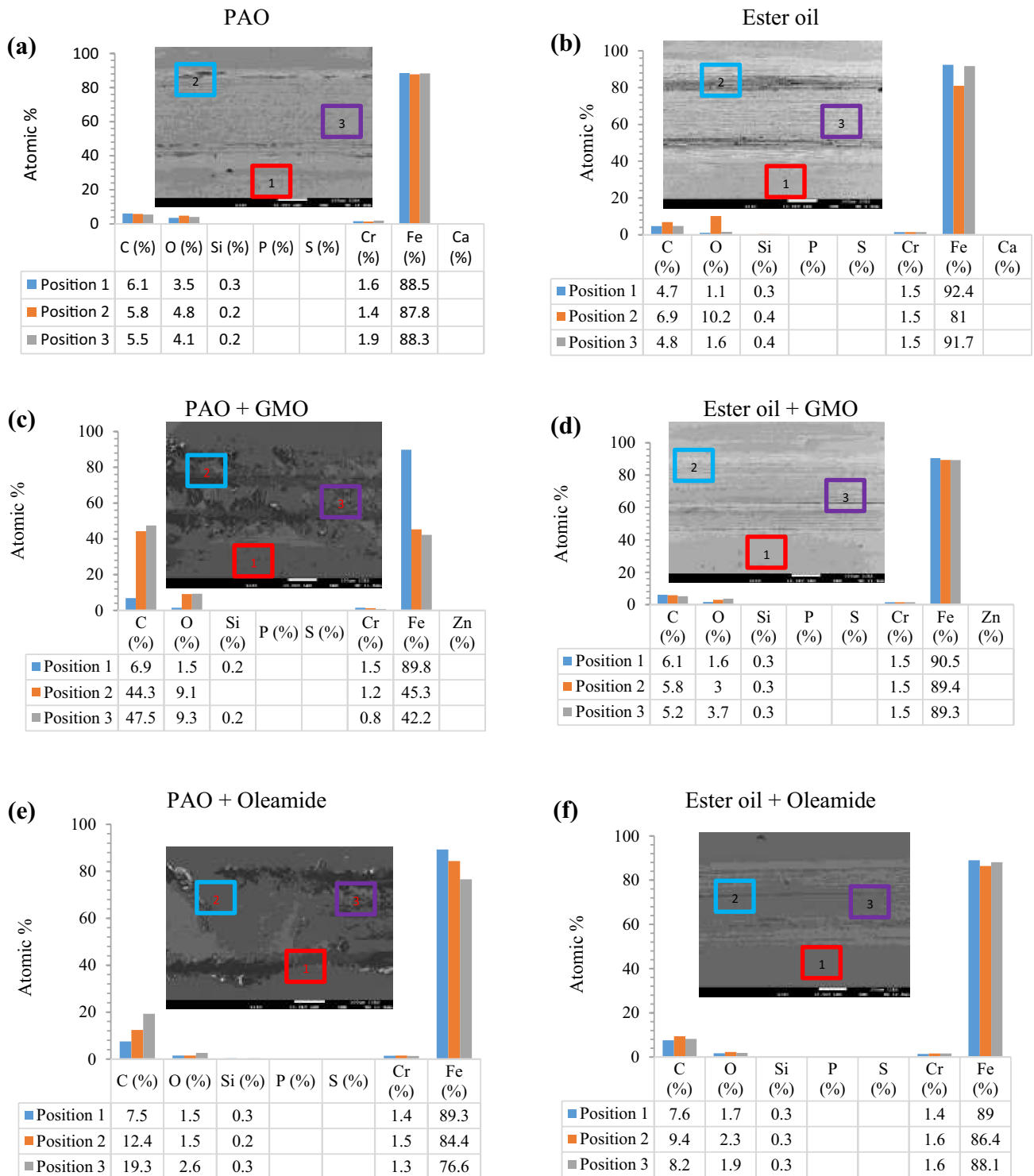
(a) PAO

	C (%)	O (%)	Si (%)	P (%)	S (%)	Cr (%)	Fe (%)	Ca (%)
Position 1	6.1	3.5	0.3			1.6	88.5	
Position 2	5.8	4.8	0.2			1.4	87.8	
Position 3	5.5	4.1	0.2			1.9	88.3	

(b) Ester oil

	C (%)	O (%)	Si (%)	P (%)	S (%)	Cr (%)	Fe (%)	Ca (%)
Position 1	4.7	1.1	0.3			1.5	92.4	
Position 2	6.9	10.2	0.4			1.5	81	
Position 3	4.8	1.6	0.4			1.5	91.7	

(c) PAO + GMO

	C (%)	O (%)	Si (%)	P (%)	S (%)	Cr (%)	Fe (%)	Zn (%)
Position 1	6.9	1.5	0.2			1.5	89.8	
Position 2	44.3	9.1				1.2	45.3	
Position 3	47.5	9.3	0.2			0.8	42.2	

(d) Ester oil + GMO

	C (%)	O (%)	Si (%)	P (%)	S (%)	Cr (%)	Fe (%)	Zn (%)
Position 1	6.1	1.6	0.3			1.5	90.5	
Position 2	5.8	3	0.3			1.5	89.4	
Position 3	5.2	3.7	0.3			1.5	89.3	

(e) PAO + Oleamide

	C (%)	O (%)	Si (%)	P (%)	S (%)	Cr (%)	Fe (%)
Position 1	7.5	1.5	0.3			1.4	89.3
Position 2	12.4	1.5	0.2			1.5	84.4
Position 3	19.3	2.6	0.3			1.3	76.6

(f) Ester oil + Oleamide

	C (%)	O (%)	Si (%)	P (%)	S (%)	Cr (%)	Fe (%)
Position 1	7.6	1.7	0.3			1.4	89
Position 2	9.4	2.3	0.3			1.6	86.4
Position 3	8.2	1.9	0.3			1.6	88.1

Fig. 5 SEM–EDX data for surfaces lubricated with base oil, GMO and oleamide. The numbers shown inside SEM images are the positions identified for EDX analysis

mostly restricted to rolling speed corresponding to mixed lubrication regime. In the boundary regime, ester oil alone offered good lubricity during the initial and final phase of rubbing. It is plausible that the low shear strength adsorbed layer formed at higher asperity junctions could have desorbed under low-speed conditions due to its inability to withstand stronger interaction from polar base oil. This might have contributed to an increase in surface shear, resulting
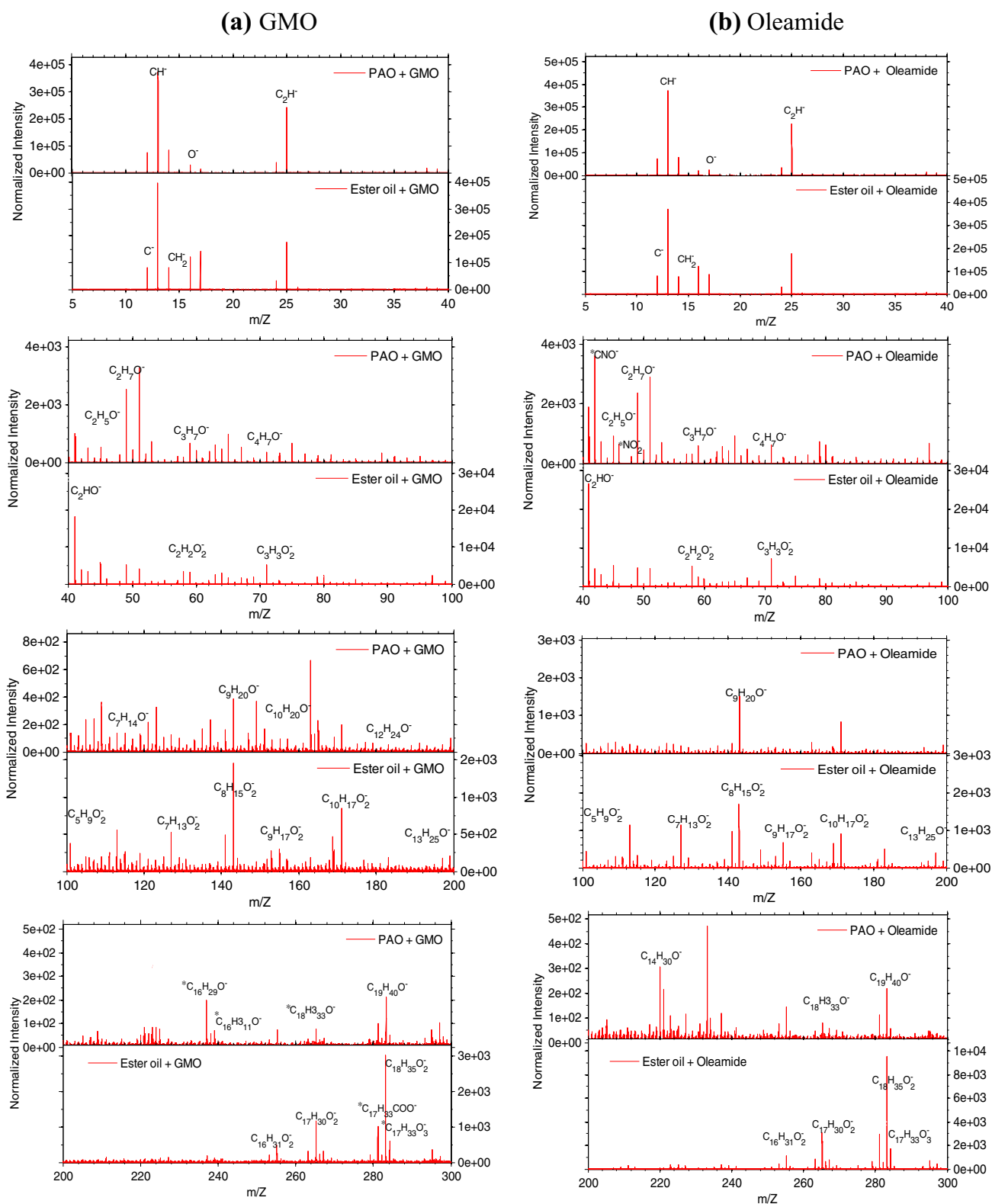
Fig. 6 Negative ion spectra of GMO and oleamide tribofilm in PAO and ester oil (* characteristic peaks of additives)

in transition of Stribeck curves to higher friction values in polar oil. From Fig. 4 it is evident that GMO exhibits superior friction reduction performance than oleamide during extended rubbing in the boundary regime. This is contrary to earlier reported work where oleamide was shown to be a more effective friction reducing agent than GMO [14, 15]. In our study the additives were subjected to harsher contact conditions ($T = 140$ ℃, SRR = 100% and Load = 36 N) than in previously reported research. Under such conditions it is likely that GMO can undergo chemical decomposition thereby yielding oleic acid and glycerol [47–50]. Glycerol decomposition was evident from ToF–SIMS analysis. It was postulated that glycerol produced by chemical decomposition of GMO can form lubricious surface films at low entrainment speeds [47]. Therefore, we hypothesize that the entrainment of lubricious glycerol into the contact led to a notable decrease in friction for GMO. Alternatively, a thicker tribofilm formed of GMO compared to oleamide (Fig. 1a and b) could have effectively reduced asperity interactions at the tribological contact leading to a reduction in BFC for GMO. It is known that OFMs with low and medium surface coverage results in high friction coefficients due to higher interdigitation with base oil [3]. On the contrary a film of high surface coverage as in case of GMO can promote slip planes during sliding with low interdigitation. All the above factors could have led to the observed frictional response.

SEM images of oleamide tribofilms formed in PAO and ester oil are shown in Fig. 5e and f, respectively. Similar to GMO, visible deposits representative of thin oleamide films are observed for PAO-based formulation. The surface formed of oleamide in polar oil appears to have horizontal scratches along the rolling direction, whereas the additive in non-polar oil resulted in a smoother surface topography. Commensurate with the observation of a visible surface film, a higher concentration of carbon and oxygen was found on the wear track for oleamide in PAO, suggestive of greater diffusivity and adsorption of the additive. A notable decrease in BFC during prolonged rubbing could be a manifestation of this behaviour. As discussed earlier, the viscous film may augment the film thickness measured between the coated glass disc and steel ball, resulting in erroneous interpretation of the measured film thickness values. However, a higher concentration of carbon and oxygen observed in PAO for both GMO and oleamide compared to in ester oil unambiguously suggests the OFMs are capable of forming thicker film in non-polar oil than in polar ones.

Positive and negative ion spectra of oleamide films formed in PAO and ester oil are shown in Fig. 6b. Peaks corresponding to molecular ions $[C_{18}H_{35}NO]^+$ with a mass of 281.48 and $C_{18}H_{35}NO + H^+$ with m/z 282.48 are observed (results not shown). Also, ions corresponding to $[CNO]^-$ (m/z 42 a.m.u.), characteristic of oleamide

fragmentation, and $[NO_2]^-$ (m/z 46 a.m.u), originated from the interaction of amide with oxidized steel surface, are observed in the negative spectrum. Here, oleamide in PAO exhibited higher peak intensity, suggesting higher surface reactivity of additive in non-polar oil than its polar counterpart does.

3.5 Influence of Base Oil on the Tribological Performance of ZDDP

ZDDP generated 20–100-nm-thick layer on the metal surface depending on the rubbing duration (Fig. 1c and d). The film formed in PAO appears to be very patchy along the rubbing direction, whereas a relatively even tribofilm was formed in ester oil (Fig. 1vii and viii). The growth of the film can be divided in to three stages. ZDDP in both oils shows an initial induction period having a slow film growth rate. This was followed by rapid film formation. During the last phase the film thickness decreased upon further rubbing. The decrease in film thickness after 30 min of rubbing in both the oils suggests that the ZDDP tribofilm is unstable and is partially lost from the surface, with the rate of decrease more pronounced in non-polar PAO oil. The thick films formed during the intermediate phase was characterized by higher friction, whereas a decrease in friction is evident for thinner films formed during prolonged rubbing. The decrease in film thickness with rubbing is contrary to resilient boundary films usually associated with ZDDP films where the decomposition products formed during rubbing are shown to accumulate on the surface [18, 51]. There is some evidence that the alkyl ZDDP structure has an effect on the rate of film formation [18]. Therefore, the inability of the additive to form a stable film during prolonged rubbing can be associated with the type of ZDDP used. It is known that amorphous ZDDP tribofilm formed during the initial phase of rubbing is relatively easily removed during rubbing [51]. Accordingly, it is hypothesized that a weaker amorphous structure is formed in PAO as compared to the more durable nanocrystalline one formed in ester oil. As ZDDP tribofilms are characterized by flat pad regions separated by deep valleys [52], it is possible that viscous film can get entrapped on the rough anti-wear film. However, unlike the OFM films, the ZDDP tribofilms did not show any interference fringes characteristic of viscous film. Earlier studies have suggested the presence of viscous layer on the top of solid-like tribofilm [53, 54]. Such deposits were also not observed in our work.

Scratches along the rolling direction are not apparent from the SLIM images. In turn, this indicates that ZDDP interacts favourably with the metal surface in both the oils providing surface protection. Theoretically, ZDDP is expected to generate thicker tribofilms in non-polar base oil as it experiences weak interactions in the bulk solution

and hence diffuse to the metal surface with little resistance [33, 34]. However, our current experimental results (optical interferograms and mean layer thickness) do not seem to corroborate this notion. Earlier studies on the influence of base oil polarity on the reaction layer thickness of AW additive was based on primary ZDDP [33, 34]. However, here we have used a mixed primary and secondary alkyl ZDDP as AW additive in the formulation. Therefore, the type of ZDDP used in the formulation might have had an effect on the film thickness. SEM images for neat base oils showed precipitate deposition which was more pronounced for ester oil (Fig. 5). Hence, it is likely that the total film thickness is the addition due to thermal degradation precipitates from the base oil and the thickness of the tribofilm from the thermal and mechanical decomposition of ZDDP. This may have contributed to a thicker tribofilm in polar oil.

The influence of rubbing time on the frictional performance of ZDDP-based oils is shown in Fig. 2g and h. Longer rubbing shifted the Stribeck curves to higher friction values for ester oil under mixed lubrication regime. However, this increase was limited to 60 min of rubbing, suggesting the contact attained a limiting surface roughness. Rubbing also contributed to an increase in friction up to 60 min for non-polar oil. However, subsequent rubbing decreased friction which can be a result of thinner tribofilm as evident from optical interferograms (Fig. 1vii) and mean central layer thickness (Fig. 1c). For both the base oils a notable increase in friction is evident at intermediate speeds than at lower speeds. The shift in friction curves at intermediate speed can be due to obstruction of lubricant entrainment into the contact by rougher solid tribofilm formed during successive rubbing [18, 28, 55]. Comparing the Stribeck curves with the tribofilm thickness, no quantitative agreement between friction and tribofilm thickness could be established, contrary to the notion that a thicker additive film results in a higher BFC. At similar rubbing durations, addition of ZDDP to both polar and non-polar oil resulted in significant increase in boundary friction (Fig. 4). The higher friction values can be attributed to the protective layer of ZDDP formed by chemical interaction with the rubbing metal surface. Interestingly, although ZDDP formed much thinner tribofilm in PAO, it resulted in higher BFC as compared to that in ester oil, which is in line with the results reported by Cen et al. [56]. But our result shows that CoF does not always increase with ZDDP film thickness. Considering that additive-free PAO exhibited a higher BFC than ester oil, this factor could also influence the frictional performance of ZDDP-based PAO.

From the SEM images (Fig. 7a and b), a notable difference in surface morphology can be observed where the ester oil-tested surface appears to be more uniform than the one tested in PAO. EDX analysis shows higher concentration of ZDDP-based elements on the surface lubricated with ester oil and such films are usually found to result in higher friction [57]. However, our results show that the thicker film formed in ester oil exhibits lower BFC compared to the film formed in PAO under similar rubbing conditions. EDX mapping analysis (results not shown) confirmed the formation of a uniform tribofilm in ester oil versus a patchy film formed on the surface lubricated with PAO. Lower BFC for ZDDP in ester oil can therefore be ascribed to the formation of a smoother and more uniformly distributed tribofilm (Fig. 1 vii and viii), as evident from SEM images and EDX mapping. It is known that alignment of phosphate chains along the rolling direction usually contributes to tribofilm of low shear strength [58]. Further, they can result in the formation of tribofilm with enhanced packing density which offers low friction [59, 60]. Therefore, it is likely that the above parameters could also have influenced the frictional performance of the anti-wear additive in PAO and ester oil.

Positive and negative ion ToF–SIMS spectra were collected to identify the chemical species on the metal surface post tribological test (Fig. 8a). Ion fragments attributed to iron were evident from the ToF–SIMS data; however, secondary ions corresponding to zinc were not observed (results not shown). This is not in agreement with the literature where zinc ions ($m/z = 64$) were detected on the surface [61, 62]. Nevertheless, our EDX data clearly showed the presence of a tribolayer rich in zinc for both PAO and ester oil. The disagreement with earlier published work can be due to the difference in ToF–SIMS technique employed in this work [61, 62]. Negative ion spectra revealed that the surface contained phosphates ($[PO_2]^-$ and $[PO_3]^-$) and pyrophosphates ($[P_2O_5]^-$), with the surface lubricated with ester oil showing a higher concentration of these products. Higher intensity peaks typical of zinc metaphosphate fragments ($[ZnP_2O_6]^-$ and $[ZnP_2O_7]^-$) are also observed where a higher concentration is found on surface lubricated with PAO oil.

To gain further insights on the chemistry of tribofilm formed of ZDDP, depth profiling was performed within the wear scar. Figure 9a and b shows the normalized intensity of selected ions as function of sputter time for surfaces lubricated with PAO and ester oil. The result suggest a film rich of zinc, phosphates and sulphate/sulphide at the top layer and higher concentration of iron near the steel substrate. A higher concentration of phosphates and sulphate/sulphide species is characteristic of tribofilm formed in ester oil. In PAO, the concentration of phosphates and sulphates exhibits a steady decrease with sputtering time, whereas in ester oil, these ions remained nearly constant for much longer time, suggesting a homogeneous film compared to the former. In PAO, iron became a dominant species after ≈ 1200 s, whereas in ester oil the steel surface/tribofilm interface was observed only after ≈ 1600 s of sputtering. Lateral distribution of selected species obtained at different depths are shown in Fig. 10a and b.
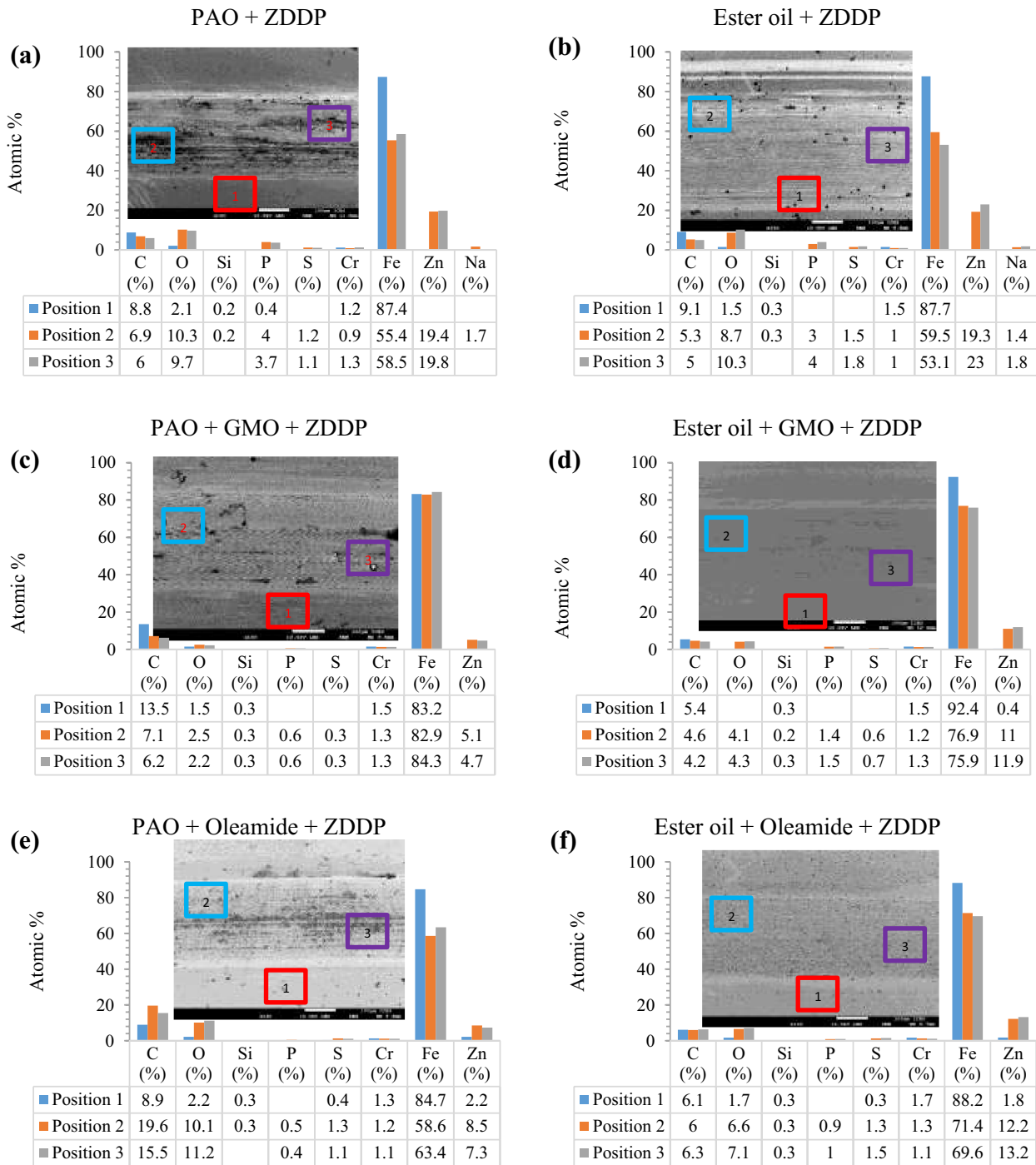
(a) PAO + ZDDP

	C (%)	O (%)	Si (%)	P (%)	S (%)	Cr (%)	Fe (%)	Zn (%)	Na (%)
Position 1	8.8	2.1	0.2	0.4		1.2	87.4		
Position 2	6.9	10.3	0.2	4	1.2	0.9	55.4	19.4	1.7
Position 3	6	9.7		3.7	1.1	1.3	58.5	19.8	

(b) Ester oil + ZDDP

	C (%)	O (%)	Si (%)	P (%)	S (%)	Cr (%)	Fe (%)	Zn (%)	Na (%)
Position 1	9.1	1.5	0.3			1.5	87.7		
Position 2	5.3	8.7	0.3	3	1.5	1	59.5	19.3	1.4
Position 3	5	10.3		4	1.8	1	53.1	23	1.8

(c) PAO + GMO + ZDDP

	C (%)	O (%)	Si (%)	P (%)	S (%)	Cr (%)	Fe (%)	Zn (%)
Position 1	13.5	1.5	0.3			1.5	83.2	
Position 2	7.1	2.5	0.3	0.6	0.3	1.3	82.9	5.1
Position 3	6.2	2.2	0.3	0.6	0.3	1.3	84.3	4.7

(d) Ester oil + GMO + ZDDP

	C (%)	O (%)	Si (%)	P (%)	S (%)	Cr (%)	Fe (%)	Zn (%)
Position 1	5.4		0.3			1.5	92.4	0.4
Position 2	4.6	4.1	0.2	1.4	0.6	1.2	76.9	11
Position 3	4.2	4.3	0.3	1.5	0.7	1.3	75.9	11.9

(e) PAO + Oleamide + ZDDP

	C (%)	O (%)	Si (%)	P (%)	S (%)	Cr (%)	Fe (%)	Zn (%)
Position 1	8.9	2.2	0.3		0.4	1.3	84.7	2.2
Position 2	19.6	10.1	0.3	0.5	1.3	1.2	58.6	8.5
Position 3	15.5	11.2		0.4	1.1	1.1	63.4	7.3

(f) Ester oil + Oleamide + ZDDP

	C (%)	O (%)	Si (%)	P (%)	S (%)	Cr (%)	Fe (%)	Zn (%)
Position 1	6.1	1.7	0.3		0.3	1.7	88.2	1.8
Position 2	6	6.6	0.3	0.9	1.3	1.3	71.4	12.2
Position 3	6.3	7.1	0.3	1	1.5	1.1	69.6	13.2

Fig. 7 SEM–EDX data for surfaces lubricated with ZDDP and binary additive system containing OFM and ZDDP. The numbers shown inside SEM images are the positions identified for EDX analysis within and outside wear scar

The images show a good agreement with the depth profile data where phosphates, sulphates, zinc and iron species are found to intergrown within the tribofilm. Comparison of total intensity along x, y suggests higher concentration of phosphates and sulphates in ester oil where it appears to be more homogeneously distributed than in PAO. This observation is in agreement with SEM–EDX and optical interferometry.

SEM and ToF–SIMS studies show the main difference between the reaction layers is with concentration and distribution of ZDDP decomposition elements. In an earlier study a difference in oxidation state of sulphur for the reaction
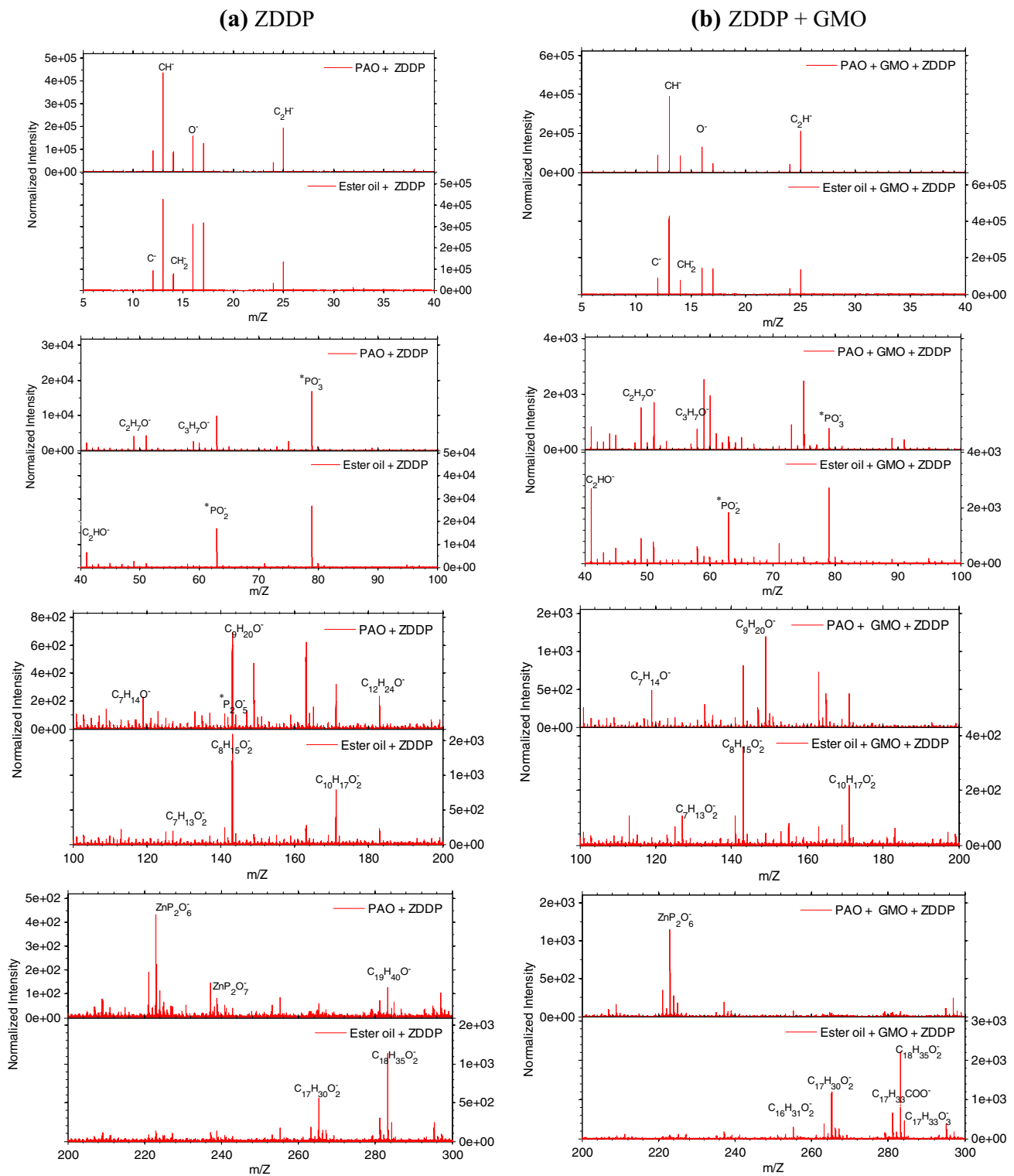
(a) ZDDP

(b) ZDDP + GMO

Fig. 8 Negative ion spectra of ZDDP and ZDDP+GMO derived tribofilm in PAO and ester oil (* characteristic peaks of additives)

layers formed of primary ZDDP in PAO and ester oil was observed using XPS [35]. Our ToF–SIMS data show PAO surface to be covered by relatively higher concentration of long-chain metaphosphates than in ester oil. The results are

in agreement with Cen et al. [56] who found phosphate chain length of ZDDP tribofilm to be longer in PAO than in ester-based oil. It is also known that short-chain phosphates and consequent nanocrystallization generally contributes to a
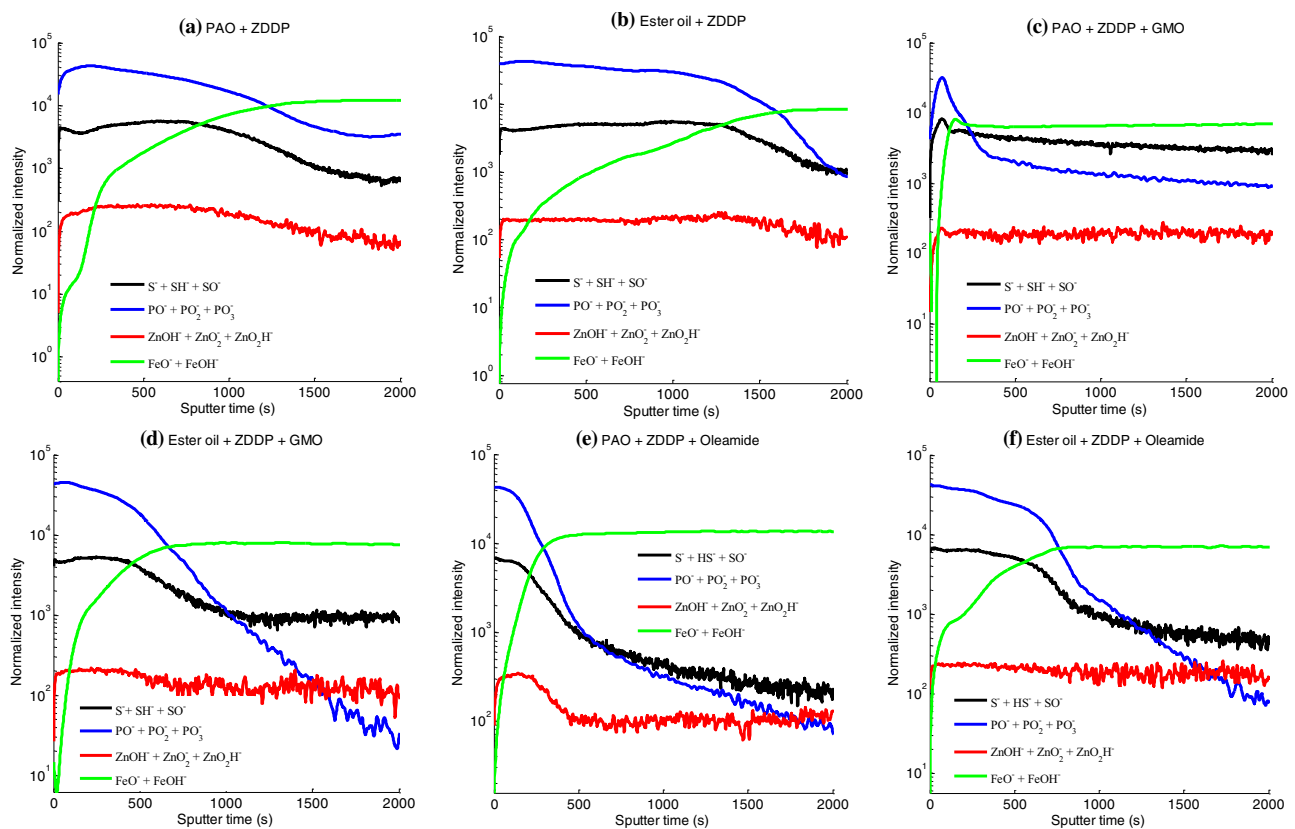
Fig. 9 Depth profile obtained on the wear track for different additives in PAO and ester oil

more resilient tribofilm than reaction layers formed of longer chains [51]. Further, the tribofilms formed by short-chain phosphates are shown to be harder than those formed by the overlying long-chain phosphates [56, 63]. With increase in hardness there can be a decrease in both the adhesive and deformation components of the measured friction coefficient [64]. Further, the long-chain phosphates with lower packing density than the shorter ones can form less compact layers [65] which may lead to higher interactions at the contact interface. This may explain why a thinner tribofilm formed in PAO contributed to a higher boundary friction coefficient than thicker film formed in ester oil.

3.6 Influence of Base Oil on the Tribological Performance of ZDDP + GMO Additive System

Optical interferograms and centre layer thickness for the binary additive system, ZDDP + GMO, in PAO and ester oil are shown in Fig. 1ix, x and c, d. A notable difference in the dynamics of tribofilm formation can be observed between the two formulations. The additives produced a thicker film in ester (polar) oil compared to PAO (non-polar oil). The thick film formed in ester oil was characterized by higher friction values than for PAO-based formulation during the

rubbing phase. In ester oil, the film thickness increased gradually with rubbing and reached a limiting thickness of ~ 100 nm at 120 min. In PAO, the film thickness increased to 64 nm after 15 min rubbing, but with further rubbing, the film thickness decreased due to desorption. While the tribofilm morphology in ester oil appears to be more uniform, a patchy film is observed in the case of PAO. Irrespective of the polarity of the base oil, marginally thicker film is exhibited by the binary additive system compared to ZDDP tribofilm during extended rubbing. Therefore, it is believed that each additive contributed to the total film thickness. This is also evident from the average friction values obtained during the rubbing phase where the friction coefficient for binary additive systems was found to lie between the values for the individual additives under similar rubbing durations.

Figure 3i and j shows the Stribeck curves acquired at different time intervals for the binary additive system in PAO and ester oil, respectively. In general, prolonged rubbing did not increase friction in the mixed lubrication regime for PAO (except for measurements after 5 min of rubbing); in contrast, an increase in friction is observed for ester oil under similar rubbing conditions. However, the increase was limited to the first 15 min of rubbing suggesting the system has attained a limiting surface roughness. A notable increase in

boundary friction is observed for the binary additive system after 5 min rubbing in ester oil. Here the BFC was found to be comparable to what was obtained for ZDDP-based ester oil (Fig. 4). On the contrary, the additives in non-polar oil led to friction reduction where the BFC was found to be lower than that of individual additives. Therefore, it is likely that during the initial phase of rubbing the frictional performance of binary additive system in ester oil is mostly governed by the properties of the anti-wear additive. On the other hand, in PAO both additives could have played a synergistic effect. Lower BFC observed during prolonged rubbing suggests that the topographical changes at the contact interface have a favourable effect on friction for both base oils. In PAO, after prolonged rubbing, the binary additive system resulted in BFC that was in between the values produced by individual additives (Fig. 4). On the contrary, in ester oil the binary additives exhibits true synergism. The contrasting behaviour suggests different reactivity between GMO and ZDDP in base oil of different polarity depending on the rubbing conditions.

SEM images show wear of varying intensities along the rolling direction (Fig. 7c and d). EDX data show a higher concentration of ZDDP-based elements (Zn, P and S) in the tribofilm formed in ester oil than in PAO. Further, compared to the single additive (ZDDP) tribofilm, a lower concentration of Zn, P and S are detected on the surface lubricated with binary additive system. These results suggest that GMO retards the formation of ZDDP tribofilm which is in agreement with previous reported research [30].

The negative ion spectra of the surfaces lubricated with GMO + ZDDP in PAO and ester oil are shown in Fig. 8b. Negative ion spectra show the surface to be composed of phosphates ($[PO_2]^-$ and $[PO_3]^-$) where the surface lubricated with ester oil shows a higher concentration of ZDDP decomposition products. However, peaks representative of long-chain metaphosphates ($[ZnP_2O_6]^-$) are only observed on the surface lubricated with PAO. $[ZnP_2O_7]^-$ peak which was more apparent for ZDDP tribofilm formed in PAO is not observed for the binary additive system. This suggests GMO to have an influence on ZDDP decomposition and film generation.

In agreement with inference drawn from EDX analysis, depth profile data (Fig. 9c and d) show lower reactivity of ZDDP decomposition products in the presence of GMO for both the oils. The profile of phosphorus and sulphate/sulphide species showed a maximum near the surface and was followed by a steady decrease in concentration of these ions. In PAO, phosphate ions reached an equilibrium concentration, whereas no such inference could be obtained for surface lubricated with ester oil. Iron appeared to be a dominant species after ≈ 150 s of sputtering for PAO, whereas for ester oil it occurred after ≈ 600 s. The intensity variations in z direction suggest higher chemical heterogeneity

for the film formed of binary additives (Fig. 10c and d). As ZDDP + GMO in PAO system had the most significant effect, it is postulated that GMO restricts the adsorption of ZDDP to a greater extent in PAO than in ester oil.

It is known that short-chain phosphates formed in ester oil generally result in lower friction than tribofilm formed of long-chain phosphates in non-polar oil. However, for the binary additive system, the concentration of Zn and P in ester oil are found to be twice of what was observed in PAO oil (from SEM–EDX). The thicker tribofilm characterized by higher concentration of ZDDP decomposition products could have led to higher BFC for the binary additive system in ester oil than for PAO (see Fig. 4).

3.7 Influence of Base Oil Polarity on Tribological Performance of ZDDP + Oleamide

The binary additive system containing oleamide and ZDDP formed a thicker film in polar ester oil in comparison to PAO (Fig. 1xi, xii and c, d). With a similar trend observed for ZDDP and ZDDP + GMO-based oils, respectively, the ability to form thick tribofilms in polar oil could be a characteristic of the type of ZDDP used in the formulation. The film formed in ester oil appears to be more homogeneous along the rubbing direction than the film formed in PAO. Horizontal scratches indicative of wear are not apparent from the optical interferograms for both the oils. In agreement with the results obtained for GMO + ZDDP-based formulation, a thicker film is exhibited by the oleamide + ZDDP system in both the oils compared to ZDDP tribofilm. This suggests each additive contributed to the total film thickness. However, unlike, a patchy/non homogeneous film observed for GMO + ZDDP system, the film formed of oleamide + ZDDP appears to be more homogeneous along the rubbing direction. Here the friction coefficient of the binary additive systems was found to be either lower than that of individual additives or to lay between the values for the individual additives depending upon the rubbing duration.

The Stribeck curves show a pronounced increase in friction with rubbing in the mixed lubrication regime (Fig. 3), whereas only a marginal difference in COF is observed for PAO and ester oil in the low-speed boundary regime. The shift in friction curves at intermediate speed can be due to obstruction of lubricant entrainment into the contact by rougher solid tribofilm formed during successive rubbing [18, 28, 55]. Comparison of Stribeck curves acquired after 5 min rubbing shows in PAO, the binary additives exhibited true synergism, whereas in ester oil the BFC was found to lie between values obtained for individual additives. However, after prolonged rubbing the BFC of the binary additives was found to be lower than that of individual additives in both PAO and ester oil. The results show that ZDDP and oleamide complement each other to varying degrees
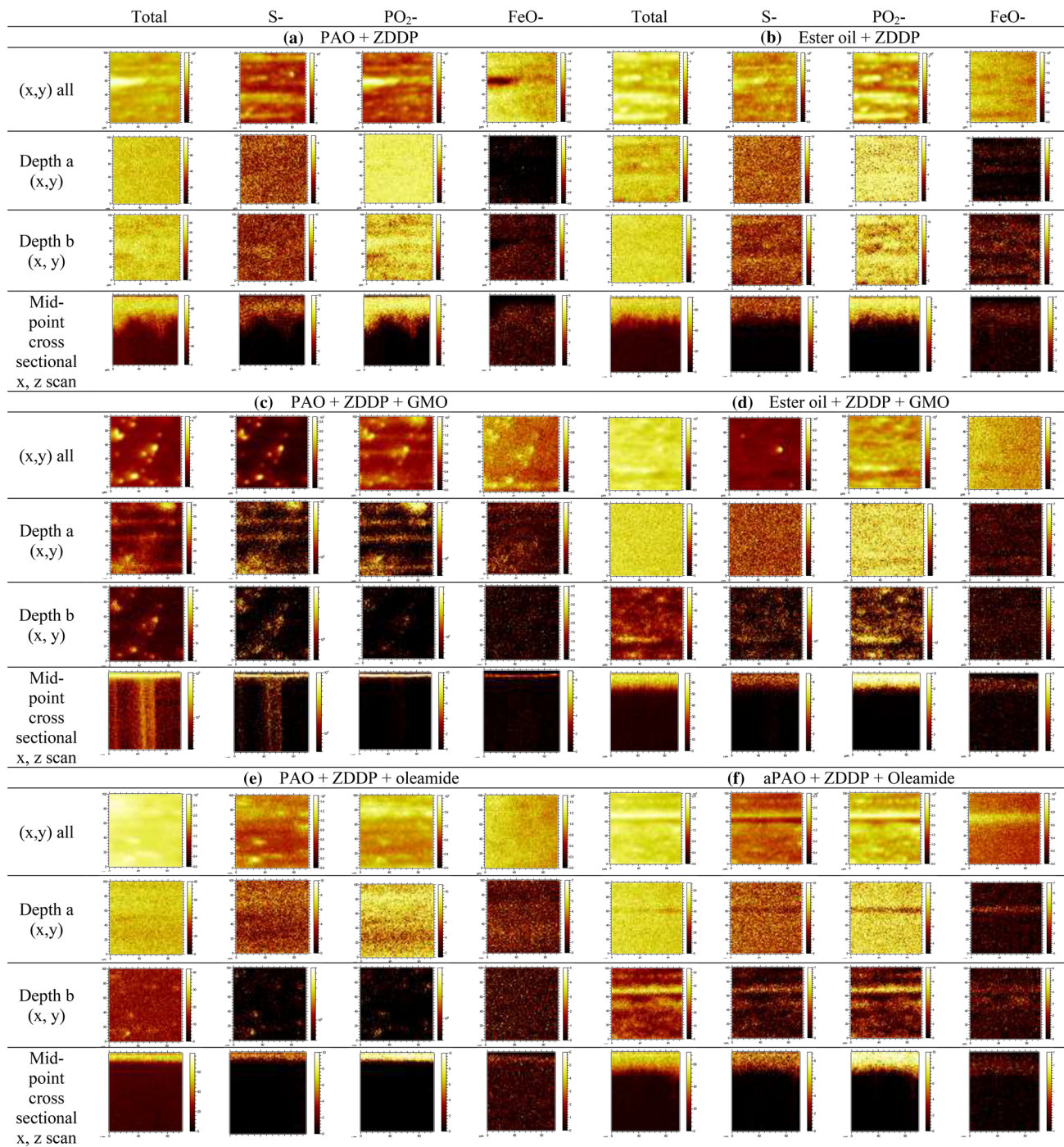
Fig. 10 3D analysis from 100×100 µm^2 analysis area of total x, y scans, at two given depth (**a**, **b**) and mid-point cross-sectional x, z scans of selected ions for different samples within wear scar

depending on the rubbing condition. Irrespective of the base oil polarity and rubbing conditions, ZDDP + oleamide systems were found to offer better friction reduction than GMO + ZDDP systems. This is despite an increase in friction observed for the ZDDP + oleamide systems during the preconditioning phase (Fig. 1). The result suggests that the

right selection of additive in the formulation is crucial for friction improvement.

SEM images show a smoother surface topography for the binary additive system compared to surfaces lubricated with ZDDP alone (Fig. 7). EDX data reveal lower concentration of ZDDP decomposition products in the presence of

oleamide where Zn and P are found to be twice higher in ester oil than in PAO. The higher amount of Zn and P within the tribofilm might have contributed to an increase in BFC in ester oil than its non-polar counterpart. Negative ion spectra of the surfaces lubricated with oleamide + ZDDP in PAO and ester oil exhibited notable difference (not shown). The distinct difference was with respect to zinc metaphosphate fragments ([ZnP_2O_6] which appeared to be found only on surface lubricated with PAO. As similar behaviour is exhibited by all formulations containing ZDDP, it is reasonable that the ability of ZDDP to form long-chain phosphates is characteristic of base oil polarity. Depth profile analysis (Fig. 9e and f) shows a steady decrease in phosphates and sulphates with sputter time for both PAO and ester oil. But, iron appeared to be a dominant species at a shorter time in PAO than surface lubricated with ester oil. It should be noted that a similar behaviour was shown by binary additive system based on ZDDP and GMO. 3D analysis of the surface suggests a more homogeneous distribution of phosphates and sulphates along x, y plane for oleamide + ZDDP than GMO + ZDDP-based system in both PAO and ester oil (Fig. 10e and f). The results are in agreement with optical interferometry, which suggest a homogeneous film along the rolling direction for oleamide + ZDDP than GMO + ZDDP system.

From EDX and ToF–SIMS it is evident that GMO restricted adsorption of ZDDP decomposition products to a greater extent than oleamide in both PAO and ester oil. Irrespective of the type of FMs, the highest reduction in ZDDP deposition was found in PAO. The results suggest the type of FMs and base oil polarity has a profound influence on reaction pathways associated with ZDDP decomposition and film generation. It is intriguing that binary additive system based on oleamide and ZDDP which had higher amount of P and Zn contributed to a lower BFC than its counterpart based on GMO with lower amount of ZDDP decomposition products. The lower friction exhibited by oleamide + ZDDP system can be due to the formation of a smoother and homogeneous tribofilm as evident from optical interferograms and ToF–SIMS 3D images. Further, this might have led to preferential alignment of phosphate chains along the rubbing direction contributing to a low shear strength tribofilm resulting in low friction.

3.8 Wear Analysis

Wear performance of the additives was evaluated by measuring the surface roughness (R_a) and wear scar width (WSW) post tribological measurements (Fig. 11). R_a measurements were performed at six random locations along the wear scar. The results show that OFMs resulted in a notable decrease in surface roughness, whereas ZDDP-based oils showed a marked increase in surface roughness. Reduced surface
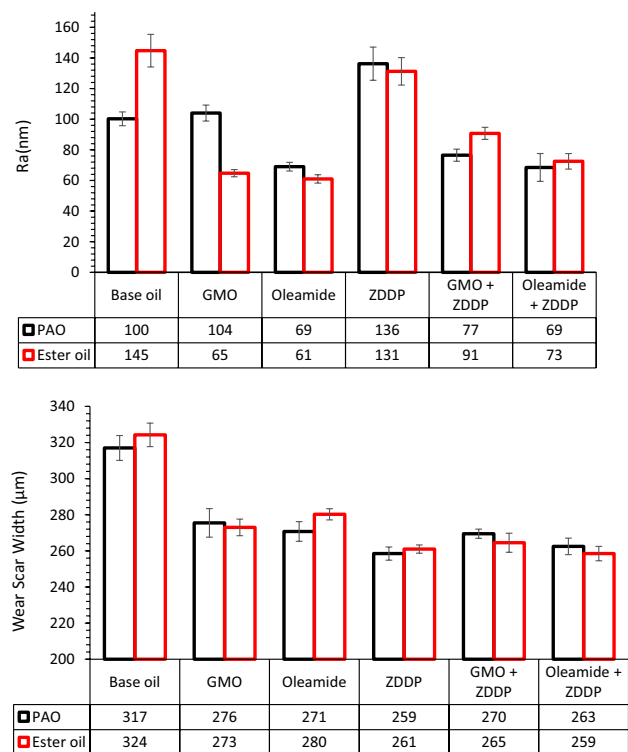

	Base oil	GMO	Oleamide	ZDDP	GMO + ZDDP	Oleamide + ZDDP
PAO	100	104	69	136	77	69
Ester oil	145	65	61	131	91	73

	Base oil	GMO	Oleamide	ZDDP	GMO + ZDDP	Oleamide + ZDDP
PAO	317	276	271	259	270	263
Ester oil	324	273	280	261	265	259

Fig. 11 Surface roughness and wear scar width for different additives in PAO and ester oil

roughness for the binary additive system suggests lower reactivity of ZDDP decomposition products on the surface. Comparing the R_a values and surface topographic images, it is hypothesized that higher surface roughness for the OFMs in PAO could be due to surface deposition of patchy additive layers. In general, the additives contributed to 13–20% decrease in wear scar width. Within experimental error, the highest reduction in wear scar width was shown by ZDDP in agreement with the formation of a thick protective film. For the binary additives, irrespective of base oil polarity, oleamide + ZDDP exhibited better wear performance than GMO + ZDDP-based systems. The higher wear resistance offered by oleamide + ZDDP also commensurate with their better frictional performance. From this study it is evident that the addition of ZDDP to OFM-based oils improves the wear performance. This is characterized by a smaller wear scar width for the binary additive systems than that for OFM-based oils. The synergistic effect of the binary additives on friction behaviour can be attributed to the improved wear performance. EDX and ToF–SIMS analyses suggest that interaction between the additives or the reaction products influenced the tribofilm formation. As rubbing is a prerequisite for producing speciation of phosphorus and sulphur [66] it is likely that ZDDP formed a thin tribolayer on the surface limiting the surface wear. This is expected to be followed by the formation of a protective multilayer comprising

both the organic friction modifier and ZDDP where each additive contributed to a different beneficial effect by outweighing the performance of individual additives.

Contrary to friction measurements, no direct correlation could be established relating base oil polarity and wear performance. It is known that formulations based on ester oil show higher wear compared to those based on non-polar oils [33, 34, 56]. In the present study we have used an ester oil of high non-polarity index (NPI = 214) which may be the reason for the lack of correlation between base oil polarity and wear.

4 Conclusions

The influence of base oil polarity on the tribological performance of OFMs (GMO and oleamide), in the absence and presence of an AW additive (ZDDP), was studied using metallocene PAO and monoester oil as representative non-polar and polar base oils. A distinct influence of base oil polarity on the particle size of dispersed phase is evident from DLS data where larger particles were observed in non-polar PAO. However, boundary friction coefficient and Z-average particle size were found to be poorly correlated.

The film thickness increased in a continual and gradual manner with rubbing for both the OFMs, resulting in decrease in friction at intermediate speeds. In general, oleamide formed a thinner film than GMO in both the oils, suggesting GMO to be a more effective surface filmforming additive than oleamide. Irrespective of the thinner film formed, oleamide-based samples offered better friction reduction than GMO-based samples during the preconditioning phase. Consistent with higher surface affinity of the OFMs in non-polar oil resulting in a thicker tribofilm, an improved friction reduction was observed in PAO during initial rubbing. Alternatively, it is reasoned that competitive adsorption between the polar OFM and base oil molecules on the metal surface led to formation of a thinner OFM film in ester oil. During extended rubbing, GMO exhibited superior friction reduction performance than oleamide. The enhanced friction reducing property of the additive could be attributed to the formation of a lubricious tribofilm comprising GMO decomposition products, as inferred from ToF–SIMS analysis of the tribofilms post friction tests. The results suggest that each additive is effective under different operating conditions. Even though OFMs were found to be effective in reducing friction at intermediate speeds, an increase in friction was observed in the low-speed regime under prolonged rubbing. It is envisaged that the transient topographical changes under harsher contact conditions resulted in higher asperity interactions, thereby reducing the effectiveness of certain OFMs.

ZDDP formed a thicker tribofilm in ester oil (compared to PAO) and lowered the boundary friction. This particular behaviour is in contrast to the notion that surface-active lubricant additives usually form a thinner tribofilm in polar base oil. ToF–SIMS data showed ester oil surface to be covered by relatively lower concentration of long-chain metaphosphates, resulting in a more resilient tribofilm than in PAO. The boundary friction coefficient (BFC) measured for the binary additive system was either lower than or between the values for the individual additives depending on the duration of rubbing. Independent of the base oil polarity and rubbing duration, the oleamide + ZDDP system offered better friction reduction than GMO + ZDDP system. Chemical composition analysis of the tribofilms indicated that the nature of base oil controlled interactions between ZDDP and OFM and consequently adsorption and reactive tribofilm formation in the boundary lubrication layer.

Surface roughness and wear scar width measured post friction test showed a greater reduction in wear for ZDDP followed by the binary additive systems, in both PAO and ester oil. The synergistic friction behaviour exhibited by the binary additive systems can be a manifestation of their improved wear performance. EDX and ToF–SIMS suggest the synergism involved interaction between the additives or its reaction products. Based on the insights from surface analysis it is hypothesized that a protective multilayer comprising both the organic friction modifier and ZDDP was formed where each additive contributed to a different beneficial effect by outweighing the performance of individual additives. However, direct correlation between base oil polarity and wear performance could not be established.

References

1. Zhang, Y., Wei, L., Hu, H., Zhao, Z., Huang, Z., Huang, A., et al.: Tribological properties of nano cellulose fatty acid esters as ecofriendly and effective lubricant additives. Cellulose **25**, 3091–3103 (2018)
2. Richardson, D.E.: Review of power cylinder friction for diesel engines. J. Eng. Gas Turbines Power **122**, 506–519 (2000)
3. Ewen, J.P., Gattinoni, C., Morgan, N., Spikes, H.A., Dini, D.: Nonequilibrium molecular dynamics simulations of organic friction modifiers adsorbed on iron oxide surfaces. Langmuir **32**, 4450–4463 (2016)

4. Jahanmir, S., Beltzer, M.: Effect of additive molecular structure on friction coefficient and adsorption. J. Tribol. **108**, 109–116 (1986)

5. Levine, O., Zisman, W.A.: Physical properties of monolayers adsorbed at the solid–air interface. I. Friction and wettability of aliphatic polar compounds and effect of halogenation. J. Phys. Chem. **61**, 1068–1077 (1957)

6. Beltzer, M., Jahanmir, S.: Effect of additive molecular structure on friction. Lubr. Sci. **1**, 3–26 (1988)

7. Ratoi, M., Anghel, V., Bovington, C., Spikes, H.: Mechanisms of oiliness additives. Tribol. Int. **33**, 241–247 (2000)

8. Allen, C., Drauglis, E.: Boundary layer lubrication: monolayer or multilayer. Wear **14**, 363–384 (1969)

9. Anghel, V., Bovington, C., Spikes, H.A.: Thick-boundary-film formation by friction modifier additives. Lubr. Sci. **11**, 313–335 (1999)

10. Cyriac, F., Tee, X.Y., Poornachary, S.K., Chow, P.S.: Influence of structural factors on the tribological performance of organic friction modifiers. Friction **9**, 380–400 (2021)

11. Kenbeek, D., Buenemann, T., Rieffe, H.: Review of organic friction modifiers-contribution to fuel efficiency? SAE Technical Paper, Place SAE Technical Paper (2000)

12. Taylor, R.I.: Tribology and energy efficiency: from molecules to lubricated contacts to complete machines. Faraday Discuss. **156**, 361–382 (2012)

13. Kenbeck, D., Bunemann, T.: Organic friction modifiers. In: Lubricant Additives: Chemistry and Applications, vol. 2 (2009)

14. Guegan, J., Southby, M., Spikes, H.: Friction modifier additives, synergies and antagonisms. Tribol. Lett. **67**, 83 (2019)

15. Miklozic, K.T., Forbus, T.R., Spikes, H.A.: Performance of friction modifiers on ZDDP-generated surfaces. Tribol. Trans. **50**, 328–335 (2007)

16. Campen, S., Green, J., Lamb, G., Atkinson, D., Spikes, H.: On the increase in boundary friction with sliding speed. Tribol. Lett. **48**, 237–248 (2012)

17. Unnikrishnan, R., Jain, M., Harinarayan, A., Mehta, A.: Additive–additive interaction: an XPS study of the effect of ZDDP on the AW/EP characteristics of molybdenum based additives. Wear **252**, 240–249 (2002)

18. Dawczyk, J., Morgan, N., Russo, J., Spikes, H.: Film thickness and friction of ZDDP tribofilms. Tribol. Lett. **67**, 34 (2019)

19. Okubo, H., Tadokoro, C., Sasaki, S.: Tribological properties of a tetrahedral amorphous carbon (ta-C) film under boundary lubrication in the presence of organic friction modifiers and zinc dialkyldithiophosphate (ZDDP). Wear **332**, 1293–1302 (2015)

20. Aktary, M., McDermott, M.T., McAlpine, G.A.: Morphology and nanomechanical properties of ZDDP antiwear films as a function of tribological contact time. Tribol. Lett. **12**, 155–162 (2002)

21. Castle, R., Bovington, C.: The behaviour of friction modifiers under boundary and mixed EHD conditions. Lubr. Sci. **15**, 253–263 (2003)

22. Ratoi, M., Niste, V.B., Alghawel, H., Suen, Y.F., Nelson, K.: The impact of organic friction modifiers on engine oil tribofilms. RSC Adv. **4**, 4278–4285 (2014)

23. Massoud, T., De Matos, R.P., Le Mogne, T., Belin, M., Cobian, M., Thiébaut, B., et al.: Effect of ZDDP on lubrication mechanisms of linear fatty amines under boundary lubrication conditions. Tribol. Int. **141**, 105954 (2020)

24. Ratoi, M., Niste, V.B., Zekonyte, J.: WS2 nanoparticles–potential replacement for ZDDP and friction modifier additives. RSC Adv. **4**, 21238–21245 (2014)

25. Dawczyk, J., Russo, J., Spikes, H.: Ethoxylated amine friction modifiers and ZDDP. Tribol. Lett. **67**, 106 (2019)

26. Dawczyk, J.U.: The effect of organic friction modifiers on ZDDP tribofilm. (2018).

27. Dobrenizki, L., Tremmel, S., Wartzack, S., Hoffmann, D.C., Brögelmann, T., Bobzin, K., et al.: Efficiency improvement in automobile bucket tappet/camshaft contacts by DLC coatings–Influence of engine oil, temperature and camshaft speed. Surf. Coat. Technol. **308**, 360–373 (2016)

28. Taylor, L., Spikes, H.: Friction-enhancing properties of ZDDP antiwear additive: part I—friction and morphology of ZDDP reaction films. Tribol. Trans. **46**, 303–309 (2003)

29. Tasdemir, H.A., Wakayama, M., Tokoroyama, T., Kousaka, H., Umehara, N., Mabuchi, Y., et al.: Ultra-low friction of tetrahedral amorphous diamond-like carbon (ta-C DLC) under boundary lubrication in poly alpha-olefin (PAO) with additives. Tribol. Int. **65**, 286–294 (2013)

30. Tasdemir, H.A., Wakayama, M., Tokoroyama, T., Kousaka, H., Umehara, N., Mabuchi, Y., et al.: Wear behaviour of tetrahedral amorphous diamond-like carbon (ta-C DLC) in additive containing lubricants. Wear **307**, 1–9 (2013)

31. Okubo, H., Watanabe, S., Tadokoro, C., Sasaki, S.: Effects of concentration of zinc dialkyldithiophosphate on the tribological properties of tetrahedral amorphous carbon films in presence of organic friction modifiers. Tribol. Int. **94**, 446–457 (2016)

32. Zhmud, B., Roegiers, M.: New base oils pose a challenge for solubility and lubricity. Tribol. Lubric. Technol. **65**, 34 (2009)

33. Tomala, A., Naveira-Suarez, A., Gebeshuber, I.C., Pasaribu, R.: Effect of base oil polarity on micro and nanofriction behaviour of base oil+ ZDDP solutions. Tribology **3**, 182–188 (2009)

34. Naveira Suarez, A., Grahn, M., Pasaribu, R., Larsson, R.: The influence of base oil polarity on the tribological performance of zinc dialkyl dithiophospate additives. Tribol. Int. **43**, 2268–2278 (2010)

35. Naveira-Suarez, A., Tomala, A., Grahn, M., Zaccheddu, M., Pasaribu, R., Larsson, R.: The influence of base oil polarity and slide–roll ratio on additive-derived reaction layer formation. Proc. Inst. Mech. Eng. J **225**, 565–576 (2011)

36. Cyriac, F., Yi, T.X., Poornachary, S.K., Chow, P.S.: Effect of temperature on tribological performance of organic friction modifier and anti-wear additive: insights from friction, surface (ToF-SIMS and EDX) and wear analysis. Tribol. Int. **157**, 106896 (2021)

37. Dowson, D., Jones, D.: Lubricant entrapment between approaching elastic solids. Nature **214**, 947–948 (1967)

38. Kaneta, M., Ozaki, S., Nishikawa, H., Guo, F.: Effects of impact loads on point contact elastohydrodynamic lubrication films. Proc. Inst. Mech. Eng. J **221**, 271–278 (2007)

39. Wu, N., Zong, Z., Fei, Y., Ma, J., Guo, F.: Thermal degradation of aviation synthetic lubricating base oil. Pet. Chem. **58**, 250–257 (2018)

40. Bhushan, B.: Frictional Heating and Contact Temperatures. Modern Tribology Handbook, Two Volume Set, pp. 257–294. CRC Press, Place CRC Press (2000)

41. Bos, J., Moes, H.: Frictional Heating of Tribological Contacts. ASME. J. Tribol. **117**(1), 171–177 (1995)

42. Feng, X., Hu, Y., Xia, Y.: Tribological research of leaf-surface wax derived from plants of Pinaceae. Lubr. Sci. **31**, 1–10 (2019)

43. Murase, A., Ohmori, T.: ToF-SIMS analysis of friction surfaces tested with mixtures of a phosphite and a friction modifier. Surf. Interface Anal. **31**, 232–241 (2001)

44. Murase, A., Ohmori, T.: ToF-SIMS analysis of model compounds of friction modifier adsorbed onto friction surfaces of ferrous materials. Surf. Interface Anal. **31**, 191–199 (2001)

45. Kano, M., Yasuda, Y., Okamoto, Y., Mabuchi, Y., Hamada, T., Ueno, T., et al.: Ultralow friction of DLC in presence of glycerol mono-oleate (GNO). Tribol. Lett. **18**, 245–251 (2005)

46. Taylor, L.J., Spikes, H.A.: Friction-enhancing properties of ZDDP antiwear additive: part II—influence of ZDDP reaction films on EHD lubrication. Tribol. Trans. **46**, 310–314 (2003)

47. Campen, S.M.: Fundamentals of organic friction modifier behaviour. (2012).

48. Tang, Z., Li, S.: A review of recent developments of friction modifiers for liquid lubricants (2007–present). Curr. Opin. Solid State Mater. Sci. **18**, 119–139 (2014)

49. Bradley-Shaw, J.L., Camp, P.J., Dowding, P.J., Lewtas, K.: Self-assembly and friction of glycerol monooleate and its hydrolysis products in bulk and confined non-aqueous solvents. PCCP **20**, 17648–17657 (2018)

50. Murgia, S., Caboi, F., Monduzzi, M., Ljusberg-Wahren, H., Nylander, T.: Acyl migration and hydrolysis in monoolein-based systems. In: Lipid and Polymer-Lipid Systems, pp. 41–46. Springer, PlaceSpringer (2002)

51. Ueda, M., Kadiric, A., Spikes, H.: On the crystallinity and durability of ZDDP tribofilm. Tribol. Lett. **67**, 123 (2019)

52. Tripaldi, G., Vettor, A., Spikes, H.: Friction behaviour of ZDDP films in the mixed, boundary/EHD regime. SAE Trans. 1819–1830 (1996)

53. Bell, J., Delargy, K.: The composition and structure of model zinc dialkyldithiophosphate anti-wear films. Proc. Eurotrib **93**, 328 (1993)

54. Bell, J., Delargy, K., Seeney, A.: Paper IX (ii) the Removal of Substrate Material Through Thick Zinc Dithiophosphate Anti-wear Films. Tribology Series, pp. 387–396. Elsevier, Place Elsevier (1992)

55. Taylor, L., Dratva, A., Spikes, H.: Friction and wear behavior of zinc dialkyldithiophosphate additive. Tribol. Trans. **43**, 469–479 (2000)

56. Cen, H., Morina, A., Neville, A.: Effect of base oil polarity on the micropitting behaviour in rolling-sliding contacts. Lubr. Sci. **31**, 113–126 (2019)

57. Mabuchi, Y., Kano, M., Ishikawa, T., Sano, A., Wakizono, T.: The effect of ZDDP additive in CVT fluid on increasing friction coefficient between belt elements and pulleys of belt-drive continuously variable transmissions. Tribol. Trans. **43**, 229–236 (2000)

58. Koike, A., Yoneya, M.: Chain length effects on frictional behavior of confined ultrathin films of linear alkanes under shear. J. Phys. Chem. B **102**, 3669–3675 (1998)

59. Lee, C., Li, Q., Kalb, W., Liu, X.-Z., Berger, H., Carpick, R.W., et al.: Frictional characteristics of atomically thin sheets. Science **328**, 76–80 (2010)

60. Lee, C., Wei, X., Li, Q., Carpick, R., Kysar, J.W., Hone, J.: Elastic and frictional properties of graphene. Phys. Status Solidi (b) **246**, 2562–2567 (2009)

61. Crobu, M., Rossi, A., Mangolini, F., Spencer, N.D.: Chain-length-identification strategy in zinc polyphosphate glasses by means of XPS and ToF-SIMS. Anal. Bioanal. Chem. **403**, 1415–1432 (2012)

62. Minfray, C., Martin, J., De Barros, M., Le Mogne, T., Kersting, R., Hagenhoff, B.: Chemistry of ZDDP tribofilm by ToF-SIMS. Tribol. Lett. **17**, 351–357 (2004)

63. Pidduck, A., Smith, G.: Scanning probe microscopy of automotive anti-wear films. Wear **212**, 254–264 (1997)

64. Mikhin, N., Lyapin, K.: Hardness dependence of the coefficient of friction. Soviet Phys. J. **13**, 317–321 (1970)

65. Brow, R.K., Tallant, D.R., Myers, S.T., Phifer, C.C.: The short-range structure of zinc polyphosphate glass. J. Non-Cryst. Solids **191**, 45–55 (1995)

66. Martin, J.M., Grossiord, C., Le Mogne, T., Bec, S., Tonck, A.: The two-layer structure of Zndtp tribofilms: Part I: AES, XPS and XANES analyses. Tribol. Int. **34**, 523–530 (2001)